

# Planar and Poly-Arc Lombardi Drawings\*

Christian A. Duncan<sup>†</sup>

David Eppstein<sup>‡</sup>

Michael T. Goodrich<sup>‡</sup>

Stephen G. Kobourov<sup>§</sup>

Maarten Löffler<sup>¶</sup>

Martin Nöllenburg<sup>||</sup>

## Abstract

In Lombardi drawings of graphs, edges are represented as circular arcs and the edges incident on vertices have perfect angular resolution. It is known that not every planar graph has a planar Lombardi drawing. We give an example of a planar 3-tree that has no planar Lombardi drawing and we show that all outerpaths do have a planar Lombardi drawing. Further, we show that there are graphs that do not even have any Lombardi drawing at all. With this in mind, we generalize the notion of Lombardi drawings to that of (smooth)  $k$ -Lombardi drawings, in which each edge may be drawn as a (differentiable) sequence of  $k$  circular arcs; we show that every graph has a smooth 2-Lombardi drawing and every planar graph has a smooth planar 3-Lombardi drawing. We further investigate related topics connecting planarity and Lombardi drawings.

## 1 Introduction

Motivated by the work of the American abstract artist Mark Lombardi [27], who specialized in drawings that illustrate financial and political networks (see Figures 1 and 2), Duncan et al. [14, 15] proposed a graph visualization style called *Lombardi drawings*. These types of drawings attempt to capture some of the visual aesthetics used by Mark Lombardi, including his use of circular-arc edges and well-distributed edges around each vertex.

A vertex with circular arc edges extending from it has *perfect angular resolution* if the smaller of the two angles between any two consecutive edges, as measured between the tangents to the circular arcs at the vertex, all have the same (arc) degree. A *Lombardi drawing* of a graph  $G = (V, E)$  is a drawing of a graph where every vertex is represented as a point, the edges incident to each vertex have perfect angular resolution, and every edge is represented as a circular arc or a line segment (i.e., a circular arc of infinite radius) between the points associated with the incident vertices of the edge.

One drawback of previous work on Lombardi drawings is that not every graph has a Lombardi drawing. In this paper we attempt to remedy this by considering drawings in which edges are represented by poly-arcs, i.e., sequences of circular arcs. This added generality will allow us to draw any graph.

Drawing planar graphs without crossings is a natural goal for graph drawing algorithms, and one that is easy to achieve when angular resolution is ignored. Lombardi himself avoided crossings in many of his drawings, as shown in Figure 1. We say that a graph is *planar Lombardi* if it has a planar Lombardi drawing. Interestingly, there are planar graphs that are not planar Lombardi [14, 17] and an immediate question is to characterize those planar graphs that are planar Lombardi. For example, it is known that trees [15], Halin graphs [14] and their generalizations called D3-reducible graphs [18], subcubic planar graphs and some (but not all) 4-regular graphs [17] are planar Lombardi. Here we continue the investigation of planar Lombardi drawings. A well-studied subclass of planar graphs are outerplanar graphs, but in terms of Lombardi drawings it remains open whether all outerplanar graphs are planar Lombardi. In this paper we show that all *outerpaths*, i.e., outerplanar graphs whose weak

\* Preliminary results contained in this paper appeared in Graph Drawing 2011 [13] and Graph Drawing 2012 [28]

<sup>†</sup> Department of Engineering, Quinnipiac University, Hamden, CT, USA

<sup>‡</sup> Department of Computer Science, University of California, Irvine, California, USA

<sup>§</sup> Department of Computer Science, University of Arizona, Tucson, Arizona, USA

<sup>¶</sup> Department of Information and Computing Sciences, Utrecht University, NL

<sup>||</sup> Algorithms and Complexity Group, TU Wien, Vienna, AT

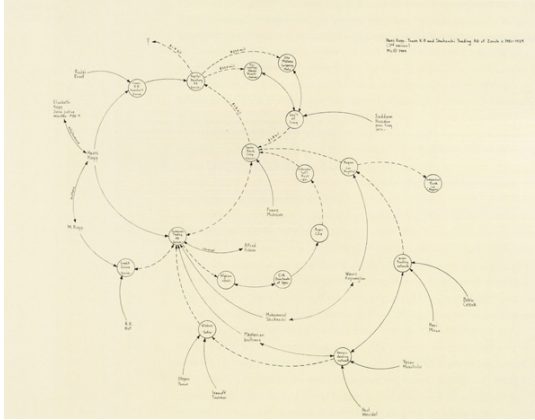


Fig. 1: Mark Lombardi, *Hans Kopp, Trans K-B and Shakarchi Trading AG of Zurich, ca. 1981–89* (3rd Version), 1999, 20.25 × 30.75 inches (cat. no. 22) [27].

Fig. 2: A portion of Mark Lombardi, *Chicago Outfit and Satellite Regimes, ca. 1931–83*, 1998, 48.125 × 96.6225 inches (cat. no. 11) [27].

<sup>24</sup> dual is a path, are planar Lombardi. Moreover, we extend our investigations to the planarity of poly-arc Lombardi drawings.

We define a *k*-Lombardi drawing to be a poly-arc drawing with at most  $k$  circular arcs per edge, with a 1-Lombardi drawing being equivalent to the earlier definition of a Lombardi drawing. We say that a *k*-Lombardi drawing is *smooth* if every edge is continuously differentiable, i.e., no edge in the drawing has a sharp bend. If a *k*-Lombardi drawing is not smooth, we say it is *pointed*. Fortunately, we do not need large values of  $k$  to be able to draw all graphs: as we show, every graph has a smooth 2-Lombardi drawing. Interestingly, this result is hinted at in the work of Lombardi himself—Figure 2 shows a portion of a drawing by Lombardi that uses smooth edges consisting of two near-circular arcs.<sup>123</sup>

**33 New Results.** In this paper we provide the following results:

- We prove that every outerpath is planar Lombardi. However, we find examples of planar 3-trees with no planar Lombardi drawing, strengthening an example from [14] of a planar graph with treewidth greater than three that is not planar Lombardi. These results are described in Section 3.
  - We find examples of graphs that do not have a Lombardi drawing, regardless of the ordering of edges around each vertex, thus strengthening an example from [14] of graphs for which a specific edge ordering cannot be drawn. In contrast, we show how to construct a smooth 2-Lombardi drawing for any graph. These results are described in Section 4.
  - We show how to represent any planar graph with a pointed 2-Lombardi planar drawing or a smooth 3-Lombardi planar drawing. These results are described in Section 5.

**43 Related Work.** In addition to the earlier theoretical work on Lombardi drawings discussed above, there is con-  
**44** siderable prior work on graph drawing with circular-arc or curvilinear edges for the sake of achieving good, but not  
**45** necessarily perfect, angular resolution [9, 22]. Confluent drawings, which use a crossing-free system of smooth  
**46** arcs and junctions (similar to train tracks) to represent non-planar graphs, have been introduced by Dickerson  
**47** et al. [12]. In a confluent drawing, two vertices are connected if and only if there exists a smooth, locally mono-  
**48** tone path between them through this system of arcs and junctions. Similarly, edge bundling [26] refers to a set of  
**49** heuristic techniques used in network visualization to reduce visual clutter by spatially grouping edges with similar

[1]: Stephen:  
get high-res  
images?

[2]: **Maarten:**  
Last time I  
searched (for a  
presentation) I  
could not find  
high quality  
images of any  
Lombardi  
drawing on the  
internet. But it  
would be great  
if we could get  
our hands on  
some!

[3]: Martin: For the first Lombardi paper we got a hi-res image from the Pierogi gallery in NYC. For the final version we can ask again about these two drawings.

50 geometric or structural properties as smooth curves. Both techniques, however, do not aim at optimizing angular  
51 resolution, but to the contrary use curvilinear arcs for merging individual edges at angles of  $0^\circ$ .

52 Brandes and Wagner [8] provided a force-directed algorithm for visualizing train schedules using Bézier curves  
53 for edges and fixed positions for vertices. Finkel and Tamassia [20] extended this work by giving a force-directed  
54 method for drawing graphs with curvilinear edges where vertex positions are not fixed. Aichholzer et al. [1] showed,  
55 for a given embedded planar triangulation with fixed vertex positions, it is possible to find a circular-arc drawing  
56 that maximizes the minimum angular resolution by solving a linear program. Chernobelskiy et al. [10] described  
57 functional Lombardi force-directed schemes, which are based on the use of dummy vertices and tangent forces,  
58 but may not always achieve perfect angular resolution. Interestingly, Efrat et al. [16] showed that, given a fixed  
59 placement of the vertices of a planar graph, it is NP-complete to determine whether the edges can be drawn with  
60 circular arcs so that there are no crossings. Thus, to the best of our knowledge, none of this related work correctly  
61 results in drawings of graphs having perfect angular resolution and curvilinear edges.

62 Graph layouts representing edges as circular or curvilinear arcs have also been investigated from a user's per-  
63 spective. Two studies compared straight-line drawings with circular-arc or curvilinear drawings [30, 31] but re-  
64 mained inconclusive in their findings; the former reports aesthetic preference for Lombardi-like layouts but worse  
65 task performance, while the latter study reports aesthetic preference for straight-line drawings. A study by Huang  
66 et al. [24] investigated the effects of curves on graph perception, when curved arcs are used to reduce edge cross-  
67 ings.

68 Alternatively, some previous work achieves good angular resolution using straight-line drawings [11, 21, 29] or  
69 piecewise-linear poly-arc drawings [19, 23, 25]. Di Battista and Vismara [11] characterized straight-line drawings  
70 of planar graphs with a prescribed assignment of angles between consecutive edges incident on the same vertex.

71 Bekos et al. [7] proposed smooth orthogonal drawings, in which every edge is a sequence of axis-aligned seg-  
72 ments and circular arc segments with common axis-aligned tangents. Such drawings are a combination of or-  
73 thogonal graph layouts and Lombardi drawings as vertices have an angular resolution of  $90^\circ$  and edges are ei-  
74 ther straight-line segments or quarter/half/three-quarter arc segments. Alam et al. [2] described an algorithm for  
75 4-planar graphs that constructs smooth orthogonal drawings with edge complexity 2, which matches the corre-  
76 sponding lower bound. Bekos et al. [6] showed how to obtain bendless smooth orthogonal drawings for special  
77 classes of 4-planar graphs, such as planar graphs of maximum degree 3. Recently, Bekos et al. [5] showed NP-  
78 hardness for a restricted version of the bendless drawing problem for smooth orthogonal drawing.

## 79 2 Preliminaries

80 In a Lombardi drawing, each vertex  $v$  has  $\deg(v)$  outgoing edges equally spaced around  $v$ . We denote the tangent  
81 vector of any such edge as the *stub* of that edge. Further, a  $k$ -*degenerate graph* is a graph that can be reduced to the  
82 empty graph by iteratively removing vertices of degree at most  $k$ .

83 Before establishing our main results, we review several useful geometric properties related to Lombardi draw-  
84 ings and circular arcs. We begin by reviewing two key properties partially established by Duncan et al. [14]:

85 **Property 2.1** ([14], Property 1). *Let  $A$  be a circular arc or line segment connecting two points  $p$  and  $q$  that both lie  
86 on circle  $O$ . Then  $A$  makes the same angle to  $O$  at  $p$  that it makes at  $q$ . Moreover, for any  $p$  and  $q$  on  $O$  and any angle  
87  $0 \leq \theta \leq \pi$ , there exist either two arcs or a line segment and pair of collinear rays connecting  $p$  and  $q$ , making angle  $\theta$   
88 with  $O$ , one lying inside and one outside of  $O$ .*

89 **Property 2.2** ([14], Property 2). *Suppose we are given two points  $p = (p_x, p_y)$  and  $q = (q_x, q_y)$  and associated angles  
90  $\theta_{ph}$  and  $\theta_{qh}$  and an angle  $\theta_{pq}$ . Consider all pairs of circular arcs that leave  $p$  and  $q$  with angles  $\theta_{ph}$  and  $\theta_{qh}$   
91 respectively (measured with respect to the positive horizontal axis) and meet at an angle  $\theta_{pq}$  in a point. The locus of  
92 meeting points for these pairs of arcs is a circle  $C$ .*

93 *Moreover, the circle  $C$  has radius  $r_c = d_{pq} \csc \alpha / 2$  and center  $(p_x + r_c \sin(\alpha + \beta), p_y - r_c \cos(\alpha + \beta))$ , where  $\alpha =$   
94  $(\theta_{ph} - \theta_{qh} - \theta_{pq})/2$ ,  $\beta$  is the angle formed by the ray from  $p$  through  $q$  with respect to the positive horizontal axis,  
95 and  $d_{pq}$  is the distance between the points  $p$  and  $q$ .*

96 *Proof.* The first part of this property was established by Duncan et al. [14]. Hence, for the remainder of the proof  
97 concerning the radius of  $C$ , we assume the reader is familiar with the arguments by Duncan et al. [14]. For simplic-

[4]: Stephen  
discuss Koebe-  
Andreev-  
Thurston  
theorem in  
related work  
and/or  
preliminaries

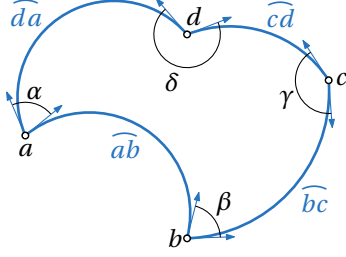


Fig. 3: An arc quadrilateral  $\diamond abcd$ .

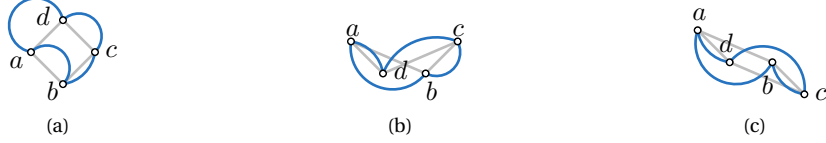


Fig. 4: (a) An arc quadrilateral without flips. (b) An arc quadrilateral with one flip. (c) An arc quadrilateral with two flips.

98      ity at the moment, let us assume that  $p$  and  $q$  are aligned horizontally, that is  $\beta = 0$ . Let  $C$  represent the circular  
 99      locus with center  $c = (x_c, y_c)$  and radius  $r_c$ . From [14] we know that the angle formed by the center of the circle and  
 100     the two points  $q$  and  $p$  is  $\angle qcp = \theta_{ph} - \theta_{qh} - \theta_{pq} = 2\alpha$ . Analyzing the isosceles triangle  $\triangle qcp$ , we determine the  
 101     radius  $r_c = d_{pq}/(2 \sin \alpha)$ .

102      Now, if  $\beta \neq 0$ , a simple rotation of  $-\beta$  about  $p$  can be applied yielding  $\alpha = \theta_{ph} - \beta - \theta_{qh} + \beta - \theta_{pq}$  and hence the  
 103     angle  $\alpha$  and the radius  $r_c$  are unaffected.

104      Using basic trigonometry and geometry, we can also determine the center of this circle as  $c = (p_x + r_c \sin(\alpha +  
 105     \beta), p_y - r_c \cos(\alpha + \beta))$ .  $\square$

106      We denote the circle  $C$  of Property 2.2 as the *placement circle* of a new vertex with respect to its neighbours  $p$   
 107     and  $q$  and the angle  $\theta_{pq}$ . An *arc quadrilateral* is a cycle consisting of four points in  $\mathbb{R}^2$ , and four arcs connecting  
 108     the points. We say an arc quadrilateral is *planar* if the arcs only intersect at the points. We denote the points by  
 109      $a$ ,  $b$ ,  $c$ , and  $d$ , and the arcs by  $\widehat{ab}$ ,  $\widehat{bc}$ ,  $\widehat{cd}$ , and  $\widehat{da}$ . Let  $\alpha$  be the angle at  $a$  between  $\widehat{da}$  and  $\widehat{ab}$ , measured counter-  
 110     clockwise. Similarly, let  $\beta$  be the angle at  $b$  between  $\widehat{ab}$  and  $\widehat{bc}$ , let  $\gamma$  be the angle at  $c$  between  $\widehat{bc}$  and  $\widehat{cd}$ , and let  $\delta$   
 111     be the angle at  $c$  between  $\widehat{cd}$  and  $\widehat{da}$ . Figure 3 shows an example.

112      **Property 2.3.** *Let  $\diamond abcd$  be an arc quadrilateral. Then  $a$ ,  $b$ ,  $c$ , and  $d$  are concyclic iff  $\alpha + \gamma - \beta - \delta = 0 \pmod{360^\circ}$ .*

113      *Proof.* Let  $\sigma = \alpha + \gamma - \beta - \delta$ . Observe that if we change the radius of an arc, say  $\widehat{ab}$ , while keeping  $a$  and  $b$  fixed,  
 114      $\alpha$  and  $\beta$  change by the same amounts. Therefore,  $\sigma$  is invariant under this operation unless a pair of arcs changes  
 115     order. When an order change does occur,  $\alpha$  (or  $\beta$ ) either changes from  $0^\circ$  to  $360^\circ$  or from  $360^\circ$  to  $0^\circ$ . Therefore,  $\sigma$   
 116      $\pmod{360^\circ}$  is invariant under any radius changes. Now, change the radii of all arcs until we obtain a straight-edge  
 117     quadrilateral  $\square abcd$ . If  $\square abcd$  is planar, it is well-known that  $a$ ,  $b$ ,  $c$ , and  $d$  are concyclic iff  $\alpha + \gamma = 180^\circ$ . Since  
 118     in this case  $\alpha + \beta + \gamma + \delta = 360^\circ$ , the claim follows. If  $\square abcd$  is not planar, assume w.l.o.g.  $\widehat{ab}$  and  $\widehat{cd}$  cross. In this  
 119     case,  $a$ ,  $b$ ,  $c$ , and  $d$  are concyclic iff  $\alpha + \gamma = \beta + \delta = 360^\circ$ ; again the claim follows.  $\square$

120      Let  $Q = \diamond abcd$  be a simple arc quadrilateral whose vertices are labeled  $a$ ,  $b$ ,  $c$ ,  $d$  in counterclockwise order. Let  
 121      $P$  be the straight-edge quadrilateral  $\square abcd$ . Then  $P$  could have the same orientation as  $Q$ , be non-simple, or have  
 122     reversed orientation, see Figure 4.

123      **Property 2.4.** *Let  $\alpha$ ,  $\beta$ ,  $\gamma$ , and  $\delta$  be four angles such that  $\sigma = \alpha + \gamma - \beta - \delta < 360^\circ$ . Let  $a$ ,  $b$ , and  $c$  be three points in  
 124     the plane on a circle  $C$ , and let  $\widehat{ab}$  and  $\widehat{bc}$  be two arcs that meet at  $b$  at an angle of  $\beta$  such that  $\widehat{ab}$  and  $\widehat{bc}$  lie on the  
 125     same side of  $C$ . Then the placement arc for  $d$  such that the four angles satisfy their specification lies on the same side  
 126     of  $C$  as  $\widehat{ab}$  and  $\widehat{bc}$ . Furthermore, there is a placement of  $d$  that results in a planar arc quadrilateral  $\diamond abcd$ .*

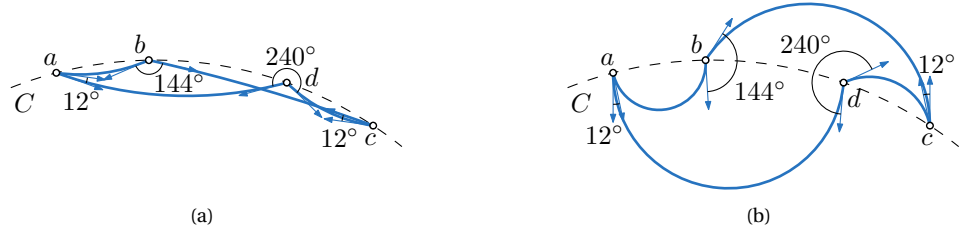


Fig. 5: If  $\sigma = 360^\circ$ , then  $a, b, c$ , and  $d$  are concyclic on  $C$ . Therefore, the arcs need to be on opposite sides of  $C$  to make a planar drawing. (a) A non-planar arc quadrilateral. (b) A planar arc quadrilateral.

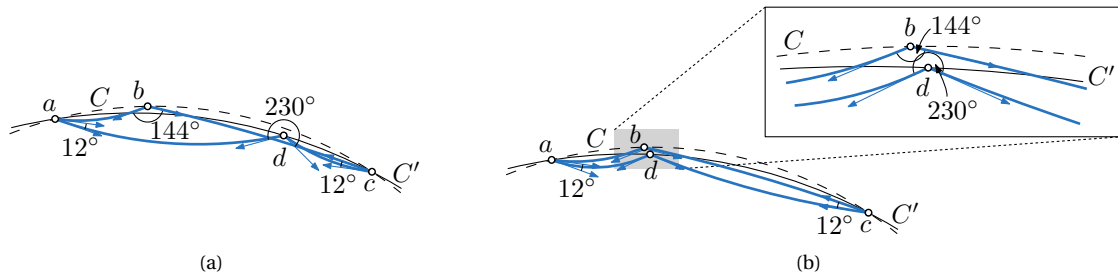


Fig. 6: If  $\sigma < 360^\circ$ , then the placement circle  $C'$  for  $d$  intersects  $C$  in  $a$  and  $c$ . (a) For some positions of  $d$  on  $C'$  the arc quadrilateral remains non-planar. (b) If  $d$  is placed on  $C'$  in between the arcs  $\widehat{ab}$  and  $\widehat{bc}$  the arc quadrilateral becomes planar.

127 *Proof.* Let  $\sigma = \alpha + \gamma - \beta - \delta$ . By Property 2.2, there is a circle of possible placements for  $d$  that satisfies the angle  
128 constraints given by  $\alpha$  and  $\gamma$ . If  $\sigma = 360^\circ$ , by Property 2.3, this circle is  $C$ . If  $\widehat{ab}$  and  $\widehat{bc}$  are on the same side of  $C$ ,  
129 then so are  $\widehat{cd}$  and  $\widehat{da}$ . Figure 5(a) illustrates this situation and  $\diamond abcd$  is non-planar for any placement of  $d$ . (Note  
130 that if  $\widehat{ab}$  and  $\widehat{bc}$  are on different sides of  $C$ , then a planar arc quadrilateral  $\diamond abcd$  exists, see Figure 5(b).) Now if  
131  $\sigma < 360^\circ$ , the placement circle  $C'$  of  $d$  is different from  $C$  and  $C'$  and  $C$  intersect in points  $a$  and  $c$ . Figure 6 depicts  
132 the situation. Placing  $d$  on  $C'$  in between the two arcs  $\widehat{ab}$  and  $\widehat{bc}$  results in a planar arc quadrilateral  $\diamond abcd$ .  $\square$

### 133 3 Planar Lombardi Drawings

134 In this section, we investigate *planar* (non-crossing) Lombardi drawings.

#### 135 3.1 A planar 3-tree with no planar Lombardi drawing

136 It is known that planar graphs do not necessarily have planar Lombardi drawings. For example, Duncan et al. [14]  
137 show that the nested triangles graph must have edge crossings whenever there are 4 or more levels of nesting.  
138 While this graph is 4-degenerate, even more constrained classes of planar graphs have no planar Lombardi draw-  
139 ings. Specifically, we can show that there exists a planar 3-tree that has no 1-Lombardi planar realization. The  
140 planar 3-trees, also known as Apollonian networks and stacked triangulations, are the planar graphs that can be  
141 formed, starting from a triangle, by repeatedly adding a vertex within a triangular face, connected to the three  
142 triangle vertices, subdividing the face into three smaller triangles. These graphs have attracted much attention  
143 within the physics research community both as models of porous media with heterogeneous particle sizes, and as  
144 models of social networks [3]. In addition, 3-trees are relevant for Lombardi drawings because they are examples  
145 of 3-degenerate graphs, which have nonplanar Lombardi drawings if vertex-vertex and vertex-edge overlaps are  
146 allowed.

[5]: Stephen  
add figure of  
that graph

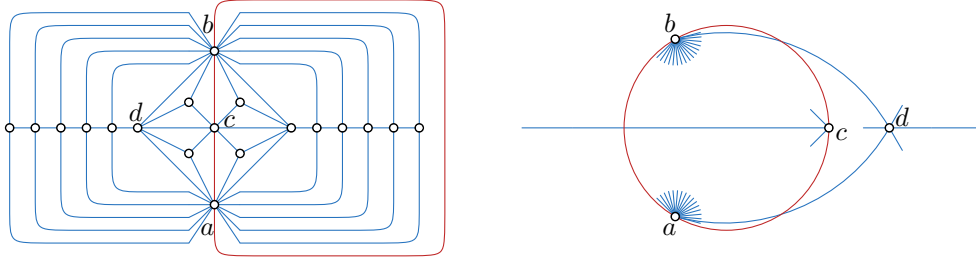


Fig. 7: Left: A planar 3-tree that has no planar Lombardi drawing. Right: For the  $K_4$  subgraph defined by the four vertices  $a$ ,  $b$ ,  $c$ , and  $d$ , a drawing with the correct angles at each vertex must necessarily have crossings.

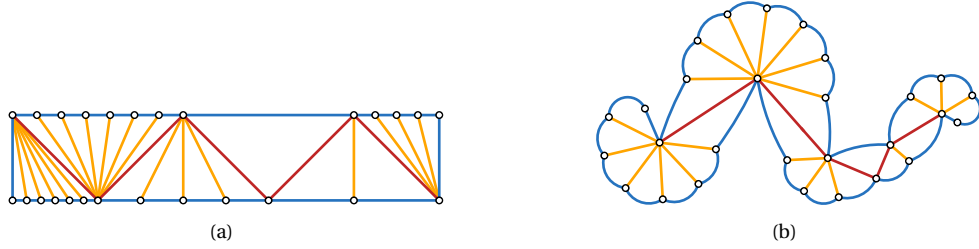


Fig. 8: (a) An outerpath. (b) A Lombardi drawing of the outerpath. The *spine* consists of the red edges, the *hull* consists of the blue edges, *petals* are yellow, and connected components of petals form *flowers*.

An example of a planar 3-tree that has no planar Lombardi drawing is given in Figure 7; in the figure, there sixteen vertices other than  $a$ ,  $b$  and  $c$ , but our construction requires a sufficient number (which we do not specify precisely) in order to force the angle between arcs  $\widehat{ad}$  and  $\widehat{ab}$  to be arbitrarily close to  $180^\circ$ . The numbers of vertices on the top and bottom of the figure should be equal. Because of this equality, the three arcs  $\widehat{ab}$ ,  $\widehat{bc}$ , and  $\widehat{ca}$  split the graph into two isomorphic subgraphs, and due to this symmetry they must meet at  $180^\circ$  angles to each other, necessarily forming a circle in any Lombardi drawing. By performing a Möbius transformation<sup>□</sup> on the drawing, we may assume without loss of generality that these three points form the vertices of an equilateral triangle inscribed within the circle, as shown in the right of the figure. Then, according to the previous analysis of 3-degenerate Lombardi graph drawing [14], there is a unique point in the plane at which vertex  $d$  may be located so that the arcs  $\widehat{ad}$ ,  $\widehat{bd}$ , and  $\widehat{cd}$  form the correct  $120^\circ$  angles to each other and the correct angles to the three previous arcs  $\widehat{ab}$ ,  $\widehat{bc}$ , and  $\widehat{ca}$ . However, as shown on the right of the figure, that unique point lies outside circle  $abc$  and causes multiple edge crossings in the drawing.

### 3.2 Outerpaths

We define an *outerpath* to be a triangulation (we later lift this restriction) of the convex hull of a set of points on two parallel lines, or equivalently to be a triangulated outerplanar graph whose weak dual (the adjacency graph of the triangular faces) is a path. Like all outerplanar graphs, outerpaths have treewidth at most two. As we now show, every outerpath is Lombardi.

The idea is to look at the ordered dual of the given outerpath  $G$ , which keeps track of left and right turns made by the dual path. Each group of consecutive turns of the same type defines a fan of triangles. We can draw the path with straight-line segments so that each  $k$ -fan corresponds to a nearly complete drawing of a regular  $k$ -gon. These  $k$ -gons are stitched together by edges whose duals correspond to edges in adjacent fans.

We define the *spine* of  $G$  to be the path connecting all vertices of degree greater than 3. We root the spine at one

<sup>□</sup> A Möbius transformation [4] is a transformation of the plane, which maps circles to circles and preserves angles. Hence a Lombardi drawing is transformed into another Lombardi drawing.

169 of its endpoints,  $v_1$ , and denote the remaining spine vertices as  $v_2, \dots, v_s$  along the rooted path. We define the *hull*  
170 of  $G$  to be the cycle bounding the outer face. Finally, we define the *petals* of  $G$  to be the remaining edges, grouped  
171 into connected components called *flowers*. Figure 8 shows an example.

172 Applying Property 2.2 along the dual path of  $G$  and drawing all petals with straight edges fixes the whole struc-  
173 ture of each flower (up to rigid transformations and scaling), with one remaining degree of freedom in the connec-  
174 tion of each pair of flowers. In Figure 8(b), we used the remaining degree of freedom to fix all spine edges to be  
175 straight-line edges as well, leading to a nice drawing. Such drawings, however, are not necessarily planar. We note  
176 that once one flower is drawn, the allowed locations of the next spine vertex lie on a circle by Property 2.2, which  
177 determines the scale of the next flower.

178 For a vertex  $v$  of  $G$ , we write  $\chi_v$  to denote its degree. For a spine vertex  $v_i$  we say that it is an *upward* (*downward*)  
179 vertex if in counterclockwise order of its neighbors  $v_{i-1}$  is the predecessor (successor) of  $v_{i+1}$ . Note that along the  
180 spine, upward and downward vertices alternate. For every vertex  $v$  we define its (spine/hull/petal) *stubs* as the  $\chi_v$   
181 equally spaced tangent vectors that describe the orientations of all incident (spine/hull/petal) edges of  $v$ .

182 The next lemma classifies the problematic quadrilaterals that can appear in outerpaths. Let  $\alpha, \beta, \gamma, \delta$  be the  
183 four inner angles of a quadrilateral and let  $\sigma = \alpha + \gamma - \beta - \delta$  as in Section 2. There are two types of quadrilaterals in  
184 outerpaths that are characterized as follows.

185 **Lemma 3.1.** *Let  $P$  be an outerpath with  $n$  vertices. Every arc quadrilateral formed by two adjacent triangles of  $P$   
186 has  $\sigma < 360^\circ$  in a planar Lombardi drawing of  $P$ , unless it is formed by one hull vertex and three consecutive spine  
187 vertices  $a, b$ , and  $c$  with  $\chi_b = 5$  and  $1/\chi_a + 1/\chi_c \leq 1/15$ .*

188 *Proof.* Let  $\diamond abcd$  be a quadrilateral with  $\sigma \geq 360^\circ$  that is part of a planar Lombardi drawing of  $P$ . Note that two of  
189 the opposite angles involved are formed by neighboring edges and thus are *Lombardi angles* (they are  $360^\circ/\chi_v$  for  
190 some vertex  $v$ ), and the other two are *double Lombardi angles* (they are  $720^\circ/\chi_v$  for some vertex  $v$ ) as they span  
191 over the diagonal of  $\diamond abcd$ . Lombardi angles are at most  $120^\circ$ , so the two Lombardi angles cannot sum to more  
192 than  $240^\circ < 360^\circ$ . So, assume w.l.o.g. that  $\alpha$  and  $\gamma$  are the double Lombardi angles and that  $\alpha + \gamma - \beta - \delta \geq 360^\circ$ . Now,  
193  $\alpha + \gamma > 360^\circ$ , since no angles are  $0^\circ$ , so at least one of  $\alpha$  or  $\gamma$  needs to be larger than  $180^\circ$ . In fact, this means one of  
194 them must be  $240^\circ$ , say  $\alpha = 240^\circ$ , and  $\chi_a = 3$ . This further implies that the two triangular faces of the quadrilateral  
195 are incident to two adjacent hull edges. Now,  $\chi_c > 3$  (unless there are only four vertices in  $G$ ), so  $\gamma \leq 180^\circ$ . If either  
196  $b$  or  $d$  has degree 3, then  $\beta$  or  $\delta$  is  $120^\circ$ , which means that  $\alpha + \gamma - \beta - \delta$  would be smaller than  $360^\circ$ . Therefore,  
197  $b, c$ , and  $d$  are all vertices of degree greater than 3, i.e., they are part of the spine. This implies  $\chi_c = 5$  (there is  
198 only one petal edge between the two spine edges, and then there are two hull edges), so  $\gamma = 144^\circ$ . This means  
199  $\beta + \delta \leq 240^\circ + 144^\circ - 360^\circ = 24^\circ$ . That is, the degrees of  $b$  and  $d$  are such that  $1/\chi_b + 1/\chi_d \leq 1/15$ .  $\square$

### 200 3.2.1 Algorithm for Planar Drawing of Outerpaths

201 The main idea for drawing an outerpath in Lombardi style is to draw the spine in an  $x$ -monotone fashion, and  
202 draw the petals in sufficiently small circles around the spine vertices so that they do not intersect each other. To  
203 this end, we align every spine vertex so that both of its spine stubs leave it at opposite angles with respect to a  
204 vertical line. This method works well as long as all spine vertices have sufficiently high degree; however, we need  
205 to abort this general scheme in several cases involving spine vertices of degree 4 or 5.

206 Our algorithm to draw outerpaths proceeds in two main phases. In the first phase, we draw the spine and  
207 all hull edges connecting two spine vertices. In the second phase we draw the flowers for each spine vertex by  
208 incrementally adding the petals. Figure 9 shows an example output as produced by the algorithm.

209 **Spine.** Let the spine vertices be  $v_1, \dots, v_s$  as they occur along the spine. We initially put vertex  $v_1$  at the origin  
210  $(0, 0)$  and rotate it so that the vertical line  $\ell_1 : x = 0$  bisects the angle between the tangents of its two incident hull  
211 edges. In all subsequent steps, the placement of the next vertex  $v_i$  depends on its degree  $\chi_{v_i}$  and the degrees of  
212 its neighbors. In the general case  $\chi_{v_i} > 5$  we place  $v_i$  on the vertical line  $\ell_i$  at distance 1 from  $v_{i-1}$  at the unique  
213 position where a circular arc from  $v_{i-1}$  tangent to the outgoing spine stub of  $v_{i-1}$  intersects  $\ell_i$  at an angle of  
214  $\pm 1.5 \cdot 360^\circ/\chi_{v_i}$  depending on whether  $v_i$  is an upward or downward spine vertex. We draw the circular arc that  
215 defined the position of  $v_i$  as the spine edge from  $v_{i-1}$  to  $v_i$ ; see Fig. 9. The same procedure still applies if  $\chi_{v_i} = 5$   
216 and  $1/\chi_{v_{i-1}} + 1/\chi_{v_{i+1}} > 1/15$ .

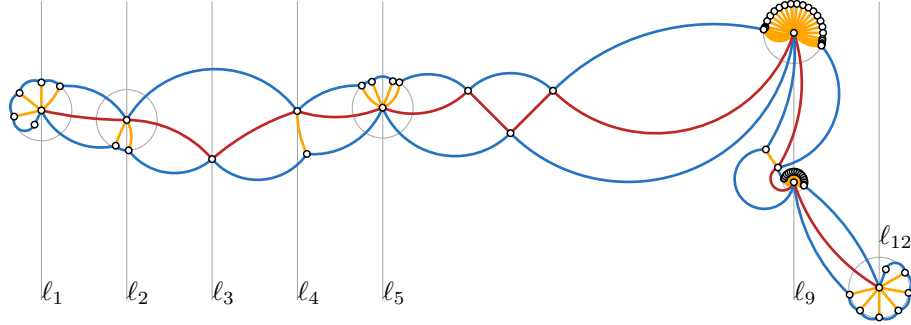


Fig. 9: A Lombardi drawing of an outerpath with spine degrees 7, 6, 4, 5, 8, 4, 4, 4, 30, 5, 30, and 9, which exhibits the different cases considered by our algorithm (we did cheat a little in that we used a larger value for  $\varepsilon$  for all vertices except  $v_{11}$ , for better visibility).

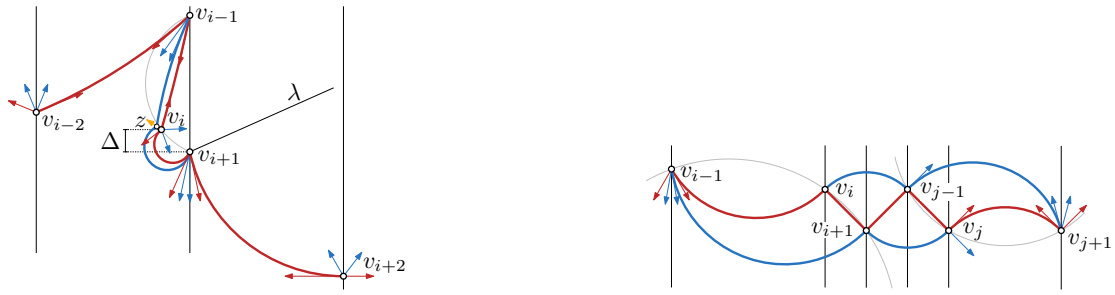


Fig. 10: Vertical placement of a degree-5 vertex  $v_i$  with two high-degree neighbors.

Fig. 11: Placement of a chain of degree-4 spine vertices  $v_i, \dots, v_j$ .

If  $\chi_{v_i} = 5$  and  $1/\chi_{v_{i-1}} + 1/\chi_{v_{i+1}} \leq 1/15$ , we switch from a horizontal placement mode to a vertical one, see Fig. 10. This is necessary to avoid edge crossings according to Lemma 3.1. The first step is to modify  $v_{i-1}$  by rotating it so that the spine stub towards  $v_i$  is left of  $\ell_{i-1}$  by  $12^\circ$ . We skip  $v_i$  for the moment and place  $v_{i+1}$  vertically above or below  $v_{i-1}$ , depending on whether  $v_{i-1}$  is a downward or upward vertex, and so that its hull stub towards  $v_{i+2}$  is vertical. If  $v_{i+1}$  is placed below  $v_{i-1}$ , the position is chosen such that there is a vertical distance of 1 to the lower of  $v_{i-1}$  and  $v_{i-2}$ ; we choose the analogous position if it is placed above  $v_{i-1}$ . Now that both  $v_{i-1}$  and  $v_{i+1}$  are placed, we construct the placement circle  $C$  for  $v_i$  based on its two spine neighbors and the angle  $\theta_{v_{i-1}v_{i+1}} = 3 \cdot 72^\circ = 216^\circ$ , see Fig. 10. We choose a position for  $v_i$  on  $C$  that has a small vertical distance  $\Delta$  from  $v_{i+1}$  (see Lemma 3.3) and connect it with two arcs to its spine neighbors. Note that this vertical structure repeats if another degree-5 vertex with the same properties follows; otherwise we continue by placing  $v_{i+2}$  horizontally to the right on a vertical line  $\ell_{i+2}$  that has the same distance to  $v_{i+1}$  as the distance between the first and third vertex of the vertical structure.

If  $\chi_{v_i} = 4$  and  $\chi_{v_{i+1}} > 4$ , we make an exception and first draw  $v_{i+1}$ , and the hull edge connecting it to  $v_{i-1}$  in this case. Vertex  $v_{i+1}$  is placed on the vertical line  $\ell_{i+1}$  at distance 2 from  $v_{i-1}$ . The position is the unique intersection point of  $\ell_{i+1}$  and the circular arc from  $v_{i-1}$  tangent to the outgoing hull stub of  $v_{i-1}$ , where the angle between the arc and  $\ell_{i+1}$  is  $\pm 0.5 \cdot 360^\circ / \chi_{v_{i+1}}$  depending on whether  $v_{i+1}$  is upward or downward. Now that  $v_{i-1}$  and  $v_{i+1}$  are both placed, we put  $v_i$  at the intersection point of the vertical line  $\ell_i$  centered between  $\ell_{i-1}$  and  $\ell_{i+1}$  and the placement circle of  $v_i$  with respect to  $v_{i-1}$ ,  $v_{i+1}$  and an enclosed angle of  $\theta_{v_{i-1}v_{i+1}} = 90^\circ$  according to Property 2.2. See vertex  $v_3$  on line  $\ell_3$  in Fig. 9 for an example.

Finally, if  $\chi_{v_i} = \dots = \chi_{v_j} = 4$  ( $i < j$ ) for a maximal sequence of  $j + 1 - i$  vertices, we place the whole sequence at once, see Fig. 11. Both the spine edge from  $v_{i-1}$  to  $v_i$  and the hull edge from  $v_{i-1}$  to  $v_{i+1}$  should intersect the vertical lines  $\ell_i$  and  $\ell_{i+1}$  at an angle of  $\pm 45^\circ$ . In order to achieve this, we place  $\ell_i$  at distance 1 from  $v_{i-1}$  and find the position of  $v_i$  as done before. Since  $v_{i+1}$  is connected by a spine edge to  $v_i$  and by a hull edge to  $v_{i-1}$  this

239 defines a placement circle for  $v_{i+1}$  and we pick the unique position for which the edge  $v_i v_{i+1}$  is straight, see Fig. 11.  
 240 Now we can draw the whole chain of degree-4 vertices in a zigzag fashion using the horizontal spacing defined by  
 241  $\ell_i$  and  $\ell_{i+1}$ . For the vertex  $v_{j+1}$  with  $\chi_{v_{j+1}} > 4$  we construct the placement circle with respect to  $v_{j-1}, v_j$ , and the  
 242 angle  $\theta_{v_{j-1}v_j} = 360^\circ/\chi_{v_{j+1}}$  and choose the position for which the angle between the vertical line  $\ell_{j+1}$  and the arc  
 243  $\overline{v_j v_{j+1}}$  is  $\pm 1.5 \cdot 360^\circ/\chi_{v_{j+1}}$ .

244 **Lemma 3.2.** *The spine does not intersect itself.*

245 *Proof.* Recall that if  $v_i$  and  $v_{i+1}$  are two vertices of degree not 5, then they are placed on vertical lines  $\ell_i$  and  $\ell_{i+1}$ .  
 246 Since the spine stub of  $v_i$  points to the right and that of  $v_{i+1}$  points to the left, the spine edge stays within this  
 247 vertical strip; clearly no two such spine edges intersect.

248 Now, let  $v_i$  be a vertex with  $\chi_{v_i} = 5$  and its spine neighbors with  $1/\chi_{v_{i-1}} + 1/\chi_{v_{i+1}} \leq 1/15$ ; they are placed on  
 249 a common vertical line  $\ell$ . Assume w.l.o.g. that  $v_{i-1}$  and  $v_{i+1}$  are upward vertices as in Fig. 10. Then both arcs  
 250  $\overline{v_{i-1}v_i}$  and  $\overline{v_iv_{i+1}}$  lie completely to the left of  $\ell$ . On the left of  $\ell$ ,  $\overline{v_{i-2}v_{i-1}}$  and  $\overline{v_iv_{i+1}}$  could intersect, but since  
 251 the left spine stub of  $v_{i-1}$  has a nonzero slope, there is a placement of  $v_i$  on its placement circle where  $\overline{v_iv_{i+1}}$  lies  
 252 completely to the right of the line supported by this stub.  $\square$

253 **Flowers.** Let  $\varepsilon' > 0$  be a number such that we can place a disk of radius  $\varepsilon'$  around every spine vertex such that  
 254 it does not intersect any spine edges other than those incident to the vertex, and such that no two such disks  
 255 intersect. Lemma 3.2 implies this number exists. To compute a suitable value for  $\varepsilon'$ , we check for each spine vertex  
 256 which spine edge is closest to it; because of the monotone structure in our construction there are only constantly  
 257 many candidates so this takes  $O(n)$  time in total. Now, for each spine vertex of degree at least 6, we preliminarily  
 258 place the two outermost petal vertices at the intersection of their placement circles and these disks of radius  $\varepsilon'$ .<sup>2</sup>  
 259 The hull edges connecting them to their neighboring spine vertices together with any hull edges that are incident  
 260 to at least one spine vertex are called the *preliminary hull*.

261 **Lemma 3.3.** *The preliminary hull edges do not have intersections with each other or the spine.*

262 *Proof.* The proof of this lemma is similar to that of Lemma 3.2, but some extra care needs to be taken. First, let  $v_i$   
 263 and  $v_{i+1}$  be two vertices of degree at least 6. Then the hull edges connecting  $v_i$  to the first petal vertex of  $v_{i+1}$  and  
 264 connecting  $v_{i+1}$  to the last petal vertex of  $v_i$  still lie completely in the vertical strip between  $\ell_i$  and  $\ell_{i+1}$ .

265 Chains of multiple vertices of degree 4 are still vertically aligned, so the same argument applies. Now, let  $v_i$  be a  
 266 degree 4 vertex with spine neighbors of degree at least 5. Then  $v_i$  could be drawn slanted. However, then  $\overline{v_{i-1}v_{i+1}}$   
 267 is the only hull edge on one side of the spine inside the vertical strip between  $\ell_{i-1}$  and  $\ell_{i+1}$ , and the two hull edges  
 268 on the other side that connect  $v_i$  to the petal vertices of  $v_{i-1}$  and  $v_{i+1}$  are adjacent and also lie within this strip. So,  
 269 they do not intersect each other either.

270 Finally, consider again the vertical case where  $v_i$  is a degree-5 vertex with spine neighbors whose degrees satisfy  
 271  $1/\chi_{v_{i-1}} + 1/\chi_{v_{i+1}} \leq 1/15$  as in Fig. 10. Let  $z$  be the single petal vertex of  $v_i$ . On the left, we first need to argue that  
 272  $\overline{zv_{i-1}}$  does not intersect any other arc. Obviously, it runs below the arc from  $v_{i-1}$  to the last petal of  $v_{i-2}$  until the  
 273 height of  $v_{i-2}$ ; thereafter it has either already reached its leftmost point and goes right towards  $v_i$  or is short enough  
 274 to not reach too far left anyway. Secondly, we need to argue that  $\overline{zv_{i+1}}$  does not intersect the leftward hull edge  
 275 emanating from  $v_{i-1}$ ; as before we can ensure this by moving the location of  $v_i$  (and therefore, also  $z$ ) sufficiently  
 276 close to  $v_{i+1}$ ; this vertical distance is denoted  $\Delta$  in the algorithm. On the right, we need to argue that the hull edge  
 277 emanating from  $v_i$  toward the flower of  $v_{i-1}$  does not intersect the leftward hull edge emanating from  $v_{i+2}$ . Since  
 278  $1/\chi_{v_{i-1}} + 1/\chi_{v_{i+1}} \leq 1/15$  we know that  $\chi_{v_{i+1}} \geq 15$  and hence the angle between two neighboring stubs of  $v_{i+1}$  is at  
 279 least  $24^\circ$ . Now, let  $\lambda$  be the line through  $v_{i+1}$  that makes an angle of  $114^\circ$  with  $\ell_{i-1}$ . If  $v_i$  is sufficiently close to  $v_{i+1}$ ,  
 280 its hull stub forms an angle of less than  $66^\circ$  with  $\ell_{i-1}$ , so its hull edge lies completely above  $\lambda$ . The angle at which  
 281 the spine arc  $\overline{v_{i+1}v_{i+2}}$  meets  $\ell_{i-1}$  is at most  $24^\circ$ ; since  $\chi_{v_{i+2}} \geq 4$  this means that the angle at which the hull edge  
 282 towards the flower of  $v_{i+1}$  comes in is at most  $90^\circ + 24^\circ = 114^\circ$ . Hence, this hull edge lies below  $\lambda$ , and the two hull  
 283 edges in the strip between  $\ell_{v_{i-1}}$  and  $\ell_{v_{i+2}}$  do not intersect.  $\square$

---

<sup>2</sup> Note that for a spine vertex of degree 5 there is a unique position for placing its only petal vertex.

284 By Lemma 3.3, the preliminary hull does not intersect itself or the spine, but it could still intersect some of the  
285  $\varepsilon'$ -disks. Therefore, we now compute a new value  $\varepsilon < \varepsilon'$  such that disks of radius  $\varepsilon$  placed at the spine vertices do  
286 not intersect any spine or hull edges. We will draw the flowers inside these  $\varepsilon$ -disks; Lemma 3.4 implies that the  
287 resulting drawing of the hull edges will still be planar after shrinking the disks to radius  $\varepsilon$ .

288 **Lemma 3.4.** *Let  $u, v$  be two adjacent spine vertices and  $w$  the first petal vertex of  $v$  (this implies that  $w$  is connected  
289 to  $u$  by a hull edge). Let  $w_1$  and  $w_2$  be two possible locations for  $w$  on its placement circle  $W$  through  $u$  and  $v$ , such  
290 that  $w_1$  lies closer to  $u$  and  $w_2$  lies closer to  $v$ . Then the hull edge connecting  $u$  to  $w_2$  lies completely inside the region  
291 bounded by  $\widehat{uv}$ ,  $\widehat{uw}_1$ , and the circle centered at  $v$  of radius  $|vw_1|$ .*

292 *Proof.* Consider the circle  $W$  of possible placements for  $w$  as shown in Fig. 12. Both  $w_1$  and  $w_2$  lie on  $W$ . The  
293 edges  $\widehat{uw}_1$  and  $\widehat{uw}_2$  both leave  $u$  in the same direction and with the same tangent. Hence, they are arcs of two  
294 touching circles, which do not intersect other than at  $u$ . Furthermore, since  $w_1$  is closer to  $u$ , the edge  $\widehat{uw}_2$  lies  
295 completely inside the region bounded by  $\widehat{uv}$ ,  $\widehat{uw}_1$ , and the circle centered at  $v$  of radius  $|vw_1|$  as claimed in the  
lemma statement.  $\square$

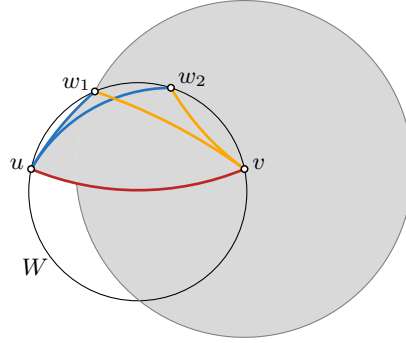


Fig. 12: Illustration for the proof of Lemma 3.4

296

297 We now describe how to draw the actual flowers recursively. Let  $C$  be a circle centered at a spine vertex  $v$ ; let  
298  $u$  and  $w$  be two points on  $C$  and let  $\widehat{uv}$  and  $\widehat{vw}$  be two arcs that lie completely inside  $C$  and have nonnegative  
299 curvature, and let  $v \geq 0$  be an integer. We will create  $v$  stubs at  $v$ , equally spaced between  $\widehat{vu}$  and  $\widehat{vw}$ , and draw  
300  $v + 2$  petal vertices (including  $u$  and  $w$ , which could be moved).

301 If  $v \geq 2$ , we keep both  $u$  and  $w$  where they are, and we proceed by drawing a circle  $D$  slightly smaller than  $C$   
302 (say, of radius  $\frac{n-1}{n}$  times smaller). By Property 2.2, there is a circle  $U$  of possible placements of the petal vertex  $u'$   
303 adjacent to  $u$ , that connects to  $v$  at the next stub and makes an angle of  $120^\circ$  at  $u'$ . Symmetrically, there is a circle  
304  $W$  of possible placements of the petal vertex  $w'$  adjacent to  $w$ . We intersect  $U$  and  $W$  with  $D$ , and place  $u'$  and  
305  $w'$  at the intersection points to the right (resp. to the left) of  $\widehat{uv}$  (resp.  $\widehat{vw}$ ). Figure 13(a) illustrates this. Now, we  
306 recurse on the smaller problem defined by  $D$ ,  $u'$ , and  $w'$ .

307 If  $v = 1$ , we simply compute the circles  $U$  and  $W$  and place the last vertex  $x$  at one of the intersection points of  
308  $U$  and  $W$ . One of the two intersection points is  $v$ ; we place  $x$  at the other one.

309 Finally, if  $v = 0$ , we cannot generally place  $u$  and  $w$  at their given location. Instead, either we fix  $u$  and place  
310  $w(u)$  at the intersection between the two placement circles based on where  $u$  is, or we fix  $w$  and place  $u(w)$  at the  
311 intersection between the two placement circles. If we fix  $u$  and  $w(u)$  is closer to  $v$  than  $w$ , we are done. Otherwise,  
312 it must be the case that if we fix  $w$  then  $u(w)$  is closer to  $v$  than  $u$  is, and we are also done. To see this, draw an arc  
313 that leaves  $u$  at the correct angle until it has the angle at which it should enter  $w$ , and vice versa; if one of these  
314 “overshoots” its target the other must “undershoot” it (refer to Figure 13(d)).

315 We apply the above algorithm to each spine vertex, choosing  $C$  to be the circle centered at  $v$  of radius  $\frac{5}{6}\varepsilon$ , and  
316 choosing  $u$  and  $w$  to be the two petal vertices we get at the intersection of  $C$  with their respective placement circles.  
317 As soon as we fix any petal vertex, we can immediately draw the hull edge connecting it to the previously fixed petal  
318 neighbor (or the spine neighbor in case of the two outermost petals).

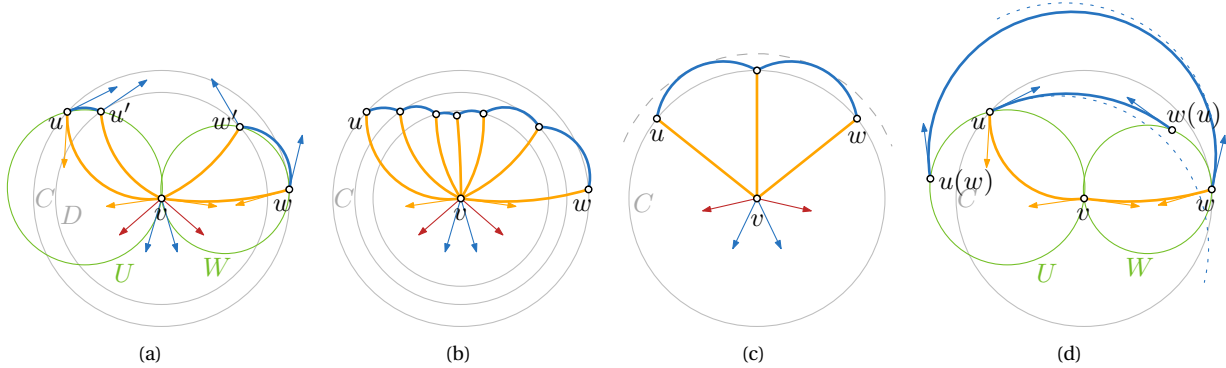


Fig. 13: (a) A partially drawn flower. (b) A possible completion of the flower. (c) In the worst case, the petals do not protrude more than a factor 1.2 out of  $C$ . (d) If Lombardi edges from  $u$  and  $w$  do not match up, then one of them overshoots the other and the other one undershoots the first (dotted).

319 The only remaining case is to draw a flower with exactly one petal. Let  $v_i$  be the spine vertex and  $w$  the adjacent  
 320 petal vertex. In this case we know that  $w$  connects to  $v_{i-1}$  and to  $v_{i+1}$  by two hull edges. We can simply intersect  
 321 the two placement circles for  $w$  and meeting angle of  $120^\circ$ , one with respect to  $v_{i-1}$  and  $v_i$ , the other with  
 322 respect to  $v_i$  and  $v_{i+1}$ . One intersection point is  $v_i$ , at the other one we place  $w$  and draw its three incident edges.  
 323 This concludes the second phase of the algorithm.

324 **Lemma 3.5.** *The flower algorithm produces an internally planar drawing that is contained within a circle of radius  
 325 at most 1.2 times bigger than  $C$ .*

326 *Proof.* For the first part of the lemma, we need to show that each time we place a petal vertex, it lies on the correct  
 327 side of the previous petal edge. In the  $v \geq 2$  case, we note that  $D$  separates  $v$  from  $u$  and  $w$ ,  $U$  passes through  $v$  and  
 328  $u$ , and  $W$  passes through  $v$  and  $w$ , so  $D$  intersects both  $U$  and  $W$ . Since the curvature of  $\widehat{uv}$  is nonnegative, there  
 329 must be at least one intersection point of  $D$  and  $U$  to the right of this arc; similarly since  $\widehat{vw}$  is non-negative there  
 330 must be at least one intersection point of  $D$  and  $W$  to the left of this arc. If the radius of  $D$  is sufficiently close to  
 331 that of  $C$ , the ordering is correct (i.e.  $u'$  lies to the left of  $w'$ ).

332 In the  $v = 1$  case, we need to use the fact that this is the last point to be placed, so the angle between  $\widehat{uv}$  and  $\widehat{vw}$   
 333 at  $v$  is at most  $2 \cdot 360^\circ / 7$ . Since the angle at  $x$  is  $240^\circ$ , and  $240 + \frac{2}{7}360 < 360$ , we clearly have  $\sigma < 360^\circ$ . When  $\chi_{v_i} = 5$   
 334 or 6, planarity is clear since there are only one or two petal vertices; if  $\chi_{v_i} = 5$ , this clearly relies on  $1/\chi_{v_{i-1}} + 1/\chi_{v_{i+1}}$   
 335 being greater than  $1/15$ .

336 Finally, we argue that this construction stays inside a circle  $C'$  of radius at most 1.2 times larger than  $C$ . We  
 337 only need to consider the arcs incident to  $u$  and  $w$ ; then the rest follow again by induction. Now, note that the  
 338 amount of protrusion of the hull edges between petal vertices depends on the outgoing angle at  $u$  (or  $w$ ), as well  
 339 as the distance to the next vertex. The outgoing angle is  $30^\circ$  in the worst case, because the curvature of  $\widehat{uv}$  is  
 340 nonnegative. The distance to the next vertex is  $360^\circ / 6$  in the worst case, because  $\chi_v \geq 6$ . The claim now follows  
 341 from basic goniometry. Figure 13(c) shows an example.  $\square$

342 Once we have placed the spine and all flowers as described above, it is clear that by construction the resulting  
 343 drawing satisfies the Lombardi properties, i.e., circular-arc edges and perfect angular resolution. The previous  
 344 lemmas prove that the drawing produced by our algorithm is indeed planar. Since every vertex is placed by com-  
 345 puting local information only, the algorithm takes linear time. We summarize the result.

346 **Theorem 3.6.** *Every outerpath has an outerplanar Lombardi drawing that can be constructed in linear time.*

347 **Non-triangulated outerpaths** The algorithm we presented assumes the input outerpath is triangulated. This is  
 348 not a restriction, as the next corollary shows.

349 **Corollary 3.7.** *Given an algorithm to draw triangulated outerpaths, we can draw any outerpath.*

350 *Proof.* For a face of size four or more we distinguish two cases. It is clear that in an outerpath there can be at most  
351 two non-hull edges in each face. If all hull edges form one connected path in the face, then we can replace this path  
352 by a single hull edge to get a triangular face and re-insert the degree-2 vertices in the end. Since that subdivides a  
353 circular arc, all angles are  $180^\circ$  as necessary.

354 If the hull edges form two disconnected paths, we temporarily remove all degree-2 vertices on the two hull  
355 paths as before. This yields a quadrilateral face  $f$  that interrupts the spine and is bounded by two hull edges and  
356 two petals. Next, we introduce a diagonal dummy spine edge  $e = uv$  that connects the left vertex  $u$  of one hull  
357 edge with the right vertex  $v$  of the other hull edge. To get the Lombardi angles right in the end, we make sure that  
358 the dummy edge does not count towards the vertex degrees  $\chi_u$  and  $\chi_v$  and hence does not affect the prescribed  
359 angles around the two vertices. The only exception is that the four angles defined by  $uv$  and the four edges of  $f$   
360 are set to  $1/2 \cdot 360^\circ / \chi_u$  and  $1/2 \cdot 360^\circ / \chi_v$ , respectively, i.e., each dummy edge bisects the two Lombardi angles on  
361 either endpoint. Hence, the drawing obtained by removing all dummy edges and re-inserting all omitted degree-2  
362 vertices is a planar Lombardi drawing of the given outerpath.  $\square$

## 363 4 *k*-Lombardi Drawings

364 In this section, we investigate *k*-Lombardi drawings. First, we establish the need to use poly-arc edges in order to  
365 be able to draw any graph.

### 366 4.1 Non-Lombardi Graphs

367 Duncan et al. [14] show a graph, Figure 14(a), for which no Lombardi drawing is possible *while preserving the given*  
368 *ordering of edges around each vertex*. However, as Figure 14(b) shows, if the ordering is not fixed, it is possible to  
369 create a valid Lombardi drawing for the graph. In this section, we provide a graph that has no Lombardi drawing  
370 *regardless of the edge ordering*.

371 There are some complications that arise when proving that a graph is non-Lombardi, compared to proving  
372 that a graph is not part of a graph class in traditional straight-line planar drawings. For example, if graph  $G$  is non-  
373 Lombardi, this does not imply that all graphs  $H \supset G$  are non-Lombardi because the addition of edges changes the  
374 angular resolution and can therefore dramatically change the subsequent placement of vertices. In addition, since  
375 the edge ordering is not fixed by the input, we must argue that any ordering forces a conflict.

376 Additional complications concern the density and symmetry of any possible counterexample. The graph in  
377 Figure 14 is 3-degenerate, and 3-degenerate graphs can be drawn Lombardi-style if we are willing to ignore vertex-  
378 vertex and vertex-edge overlaps [14] (as shown in Figure 14(a)). Consequently, if a 3-degenerate graph is to be  
379 a counterexample, we must show that all vertex orderings force at least two vertices to overlap. Intuitively, 4-  
380 degenerate graphs should be more restrictive, but the simplest 4-degenerate graph,  $K_5$ , nevertheless has a circular  
381 Lombardi drawing. One issue is the fact that  $K_5$  is extremely symmetrical. Therefore, we shall modify this graph  
382 to break its symmetry. We define our counterexample graph  $G_8$  to be  $K_5$  with the addition of three degree-one  
383 vertices causing one of the vertices of the original  $K_5$  to have degree 5 and another to have degree 6, while the  
384 other three remain with degree 4; see Figure 15(a).

#### 385 4.1.1 Proof of non-Lombardiness

386 **Theorem 4.1.** *The graph  $G_8$  is non-Lombardi.*

387 *Proof.* Let  $v_0, v_1, v_2$  be the three vertices of  $G_8$  with degree four. Let  $v_3$  and  $v_4$  be the vertices with degree five  
388 and six, respectively. We do not care about the final placement of the degree-one vertices, whose main purpose  
389 is to alter the angular resolution of  $v_3$  and  $v_4$ . Using a Möbius transformation we can assume that the first three  
390 vertices  $v_0, v_1$ , and  $v_2$  are placed on the corners of a unit equilateral triangle such that  $v_0$  and  $v_1$  have positions  
391  $(0, 0)$  and  $(1, 0)$  respectively. We shall show that for every edge ordering, the two vertices  $v_3$  and  $v_4$  cannot both be  
392 placed to maintain correctly their angular resolution and be connected to each other. We do this by establishing

[6]: Stephen:  
why not use  
notion of  
embedding?

[7]: Maarten:  
How exactly  
would you  
define an  
embedding  
then? Usually it  
either means  
“combinatorial  
embedding”,  
which only  
makes sense for  
planar  
(drawings of)  
graphs, or  
“geometric  
embedding” in  
the sense of the  
whole map  
from the graph  
to the plane.  
For  
straight-line  
drawings this is  
reasonable,  
since a  
mapping from  
the vertices  
induces a  
mapping from  
the edges (and  
you can loosely  
use  
“embedding” to  
mean “order  
type”), but  
when edges are  
not straight this  
seems less  
useful to me.

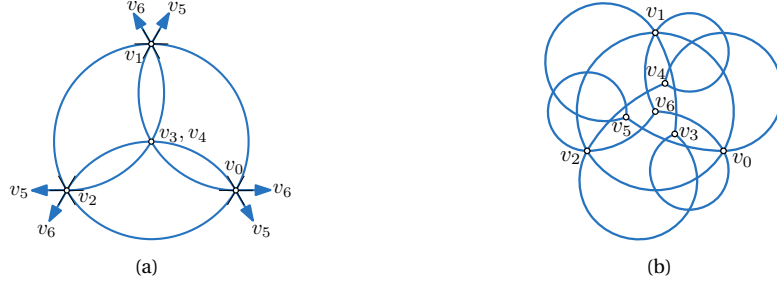


Fig. 14: A 7-vertex 3-degenerate graph that has no Lombardi drawing with the given edge ordering. (a) A Möbius transformation makes one triangle equilateral, forcing the other 4 vertices to be placed at the centroid and the point at infinity; (b) A different ordering that does provide a Lombardi drawing.

393 the algebraic equations for their positions based on the edge orderings of all vertices. We then show that such a set  
394 of equations has no solution for any valid assignment of orderings.

We first establish a notation for representing a specific edge ordering. For every vertex  $v_i$  with neighbor  $v_j$ , let  $k_{ij}$  represent the cyclic ordering of edge  $(v_i, v_j)$  about  $v_i$  with  $k_{01} = 0$  and  $k_{i0} = 0$  for  $i > 0$ . For example, in Figure 15(a), the edge ordering around  $v_4$  has  $k_{41} = 2$ ,  $k_{42} = 4$ ,  $k_{43} = 5$ ,  $k_{46} = 1$ , and  $k_{47} = 3$ . The *twist*  $\varphi_i$  of a vertex  $v_i$  is the angle made by the arc extending from  $v_i$  to the neighbor  $v_j$  with  $k_{ij} = 0$ . From the initial placement of  $v_0, v_1$ , and  $v_2$  on an equilateral triangle and their respective edge orderings, we can uniquely determine the twists for each of these vertices; see Figure 15(b). Since the three vertices lie on an equilateral triangle, the tangents to the circle defined by the three points also form an equilateral triangle. From Property 2.1, the angles formed by the arcs connecting each pair of vertices to the tangents at the circle yield matching (but undetermined) angles, labeled  $\psi_a, \psi_c$ , and  $\psi_e$ . The angles  $\psi_b, \psi_d$ , and  $\psi_f$  are determined uniquely by the edge orderings as follows:

$$\psi_b = 2\pi - k_{02}\pi/2 \quad (1)$$

$$\psi_d = k_{12}\pi/2 \quad (2)$$

$$\psi_f = 2\pi - k_{21}\pi/2 \quad (3)$$

Noting that certain triplets of angles yield a value of  $\pi$  modulo  $2\pi$ , we have the following three equations with  $i_0, i_1, i_2 \in \{0, 1\}$ :

$$\psi_a + \psi_b + \psi_c = \pi + 2i_0\pi \quad (4)$$

$$\psi_c + \psi_d + \psi_e = \pi + 2i_1\pi \quad (5)$$

$$\psi_e + \psi_f + \psi_a = \pi + 2i_2\pi. \quad (6)$$

Solving for  $\psi_a$  yields:

$$\begin{aligned} (\psi_a + \psi_b + \psi_c) - (\psi_c + \psi_d + \psi_e) + (\psi_e + \psi_f + \psi_a) &= (\pi + 2i_0\pi) - (\pi + 2i_1\pi) + (\pi + 2i_2\pi) \\ 2\psi_a + \psi_b - \psi_d + \psi_f &= 2\pi + 2(i_0 - i_1 + i_2)\pi \\ 2\psi_a &= \pi - \psi_b + \psi_d - \psi_f + 2(i_0 - i_1 + i_2)\pi. \end{aligned} \quad (7)$$

For the twist for  $v_0$ , we wish to know the value of  $\xi$ , the angle for the arc from  $v_0$  to  $v_1$ . Noting that  $\xi = \psi_a + \psi_b + 2\pi/3 - 2i_0\pi$  and substituting in Equations (1-3) with Equations (7) yields

$$\begin{aligned} 2\xi &= 2\psi_a + 2\psi_b + 4\pi/3 - 4i_0\pi \\ 2\xi &= (\pi - \psi_b + \psi_d - \psi_f + 2(i_0 - i_1 + i_2)\pi) + 2\psi_b + 4\pi/3 - 4i_0\pi \\ 2\xi &= 7\pi/3 + \psi_b + \psi_d - \psi_f + 2(i_2 - i_0 - i_1)\pi \\ 2\xi &= 7\pi/3 + (2\pi - k_{02}\pi/2) + (k_{12}\pi/2) - (2\pi - k_{21}\pi/2) + 2(i_2 - i_0 - i_1)\pi \\ 2\xi &= 7\pi/3 + (k_{12} + k_{21} - k_{02})\pi/2 + 2(i_2 - i_0 - i_1)\pi \\ \varphi_0 &= \xi = 7\pi/6 + (k_{12} + k_{21} - k_{02})\pi/4 + (i_2 - i_0 - i_1)\pi. \end{aligned} \quad (8)$$



Fig. 15: (a)  $G_8$  with  $K_5$  part drawn Lombardi-style and additional edges shown. (b) Computing the twist for the three vertices 0, 1, and 2. The twist for vertex 0 is  $\xi$ .

Noting that  $\varphi_0 + \psi_c + \pi/3 = 2\pi$  yields  $\varphi_1 = \pi - \varphi_0$ . Similarly,  $\varphi_2 = \pi - \psi_a = 5\pi/3 - \varphi_0 - k_{02}\pi/2 + 2(1 - i_0)\pi$ .  
The positions and orienting twists of the first three vertices also yield a unique position and twist for vertices  
 $v_3$  and  $v_4$ . After determining these values, we shall show that in all orderings it is not possible to connect  $v_3$  to  $v_4$   
with a single circular arc while still maintaining the proper angular resolution.

From Property 2.2,  $v_3$  must lie on a circle  $C_{01}$  defined by the neighbors  $v_0$  and  $v_1$  and their corresponding arc tangents. Similarly, it must lie on circles  $C_{02}$  and  $C_{12}$ . The intersection of these three circles determines the position and orientation of  $v_3$ . Let us proceed to determine  $C_{01}$ . Letting  $p = v_0$  and  $q = v_1$ , we have  $\theta_{ph} = \varphi_0 + \pi k_{03}/4$  and  $\theta_{qh} = \varphi_1 + \pi k_{13}/4$  and  $\theta_{pq} = \pi(k_{31} - k_{30})/5 = \pi k_{31}/5$ . From Property 2.2 and the fact that  $d_{pq} = 1$ , we can determine that  $C_{01}$  has radius  $r_{01} = \csc \alpha_{01}/2$  and center  $c_{01} = (r_{01} \sin \alpha_{01}, -r_{01} \cos \alpha_{01}) = (1/2, -\cot \alpha_{01}/2)$  with  $\alpha_{01} = (\theta_{ph} - \theta_{qh} - \theta_{pq})/2 = \varphi_0 - \pi/2 + \pi(5k_{03} - 5k_{13} - 4k_{31})/40$ . Similarly,  $C_{02}$  has radius  $r_{02} = \csc \alpha_{02}/2$  and center  $c_{02} = (r_{02} \sin(\alpha_{02} + \pi/3), -r_{02} \cos(\alpha_{02} + \pi/3))$  with  $\alpha_{02} = \varphi_0 - 5\pi/6 + \pi(5k_{03} + 10k_{02} - 5k_{23} - 4k_{32})/40 + (i_0 - 1)\pi$ .

Given the circles and the position of  $v_0$  at the origin, it is easy to determine the intersection of the two circles, one of which is  $v_0$  and the other, if it even exists, must be  $v_3$ . Since  $v_0$  must lie on the intersection, the line from  $v_0$  to  $v_3$  is perpendicular to the line,  $\ell$ , through the two centers. Moreover,  $v_3$  is the reflection of  $p$  about  $\ell$ . Thus, letting  $\vec{v} = (v_x, v_y) = c_{02} - c_{01}$ ,  $\vec{c} = v_0 - c_{01} = -c_{01}$ , and  $\vec{v}^\perp = (-v_y, v_x)$  yields

$$v_3 = \frac{-2\vec{c} \cdot \vec{v}^\perp}{\vec{v} \cdot \vec{v}} \vec{v}^\perp. \quad (9)$$

To establish the twist  $\varphi_3$  at  $v_3$  we observe from Property 2.1 that the angle  $\alpha$  formed by the line  $\ell_{03}$  from  $v_0$  to  $v_3$  and the tangent of the curve from  $v_0$  to  $v_3$  is the same as the tangent of the curve from  $v_3$  to  $v_0$  and the line  $\ell_{03}$ . Moreover,  $\theta_{03} = \varphi_0 + k_{03}\pi/4 = \alpha + \beta_{03}$  and  $\varphi_3 = \theta_{30} = \pi - \alpha + \beta_{03}$  where  $\beta_{03} = \arctan(v_3(y)/v_3(x))$  is the slope of  $\ell_{03}$ . From this, we can deduce that  $t_3 = \pi - t_0 - k_{03}\pi/4 + 2\beta_{03}$ . The exact same calculations can be used to compute  $v_4$  and  $t_4$ .

As with the twists for  $t_3$  and  $t_4$ , we can use Property 2.1 to determine the angles formed by the arc from  $v_3$  to  $v_4$  given their positions and twists. We know that the angles of the tangents to the arc at  $v_3$  and  $v_4$  are  $\theta_{34} = t_3 + k_{34}\pi/5$  and  $\theta_{43} = t_4 + k_{43}\pi/6$  respectively. Letting  $\beta_{34} = \arctan((v_4(y) - v_3(y))/(v_4(x) - v_3(x)))$  be the slope of the line from  $v_3$  to  $v_4$ , we have that  $\theta_{34} - \beta_{34} = \alpha$  and  $\pi - \alpha = \theta_{43} - \beta_{34}$ . Consequently, we have

$$\theta_{34} + \theta_{43} = \pi + 2\beta_{34}. \quad (10)$$

Each specific edge ordering therefore yields a unique set of positions and twists for  $v_3$  and  $v_4$  as outlined above. To show that no Lombardi drawing is possible one must simply show that Equation 10 does not hold for *any* edge ordering. Though there are a finite number of possible orderings and though symmetries could be used to reduce that number, the individual case analysis for such a proof appears to be quite unwieldy. Instead, we simply iterate over every possible edge ordering, applying these equations to a numerical algorithm that searches for a valid non-contradictory assignment. The Python code for this program is shown in Table 1. As can be seen from the code, it verifies using floating-point calculations with 100-bit precision that each edge ordering has angles that are farther than  $\epsilon = 10^{-6}$  from satisfying Equation 10. By running this program, one can see that no valid assignments are possible concluding our proof.  $\square$

```

#!/usr/bin/python

from itertools import *
from bigfloat import *

def match(k0,k1,k2,k3,k4,i0,i1,i2):
    (k01,k02,k03,k04)=(0,k0[0],k0[1],k0[2])
    (k10,k12,k13,k14)=(0,k1[0],k1[1],k1[2])
    (k20,k21,k23,k24)=(0,k2[0],k2[1],k2[2])
    (k30,k31,k32,k34)=(0,k3[0],k3[1],k3[2])
    (k40,k41,k42,k43)=(0,k4[0],k4[1],k4[2])
    b,d,f = 2 - k02/2.0, k12/2.0, 2-k21/2.0          # Eqs 1-3
    t0 = 7.0/6.0 + (k12 + k21 - k02)/4.0 + (i2-i0-i1) # The twists

    # Compute v3 and t3
    a01 = t0 - 0.5 + (5*k03 - 5*k13 - 4*k31)/40.0
    a02 = t0 + i0-11.0/6.0 + (5*k03 + 10*k02 - 5*k23 - 4*k32)/40.0
    r01, r02 = 0.5/sin(a01 * const_pi()), 0.5/sin(a02 * const_pi())
    c01 = (0.5, -0.5/tan(a01*const_pi()))
    c02 = (r02*sin((a02 + 1.0/3.0)*const_pi()), -r02*cos((a02 + 1.0/3.0)*const_pi()))
    v = (c02[0] - c01[0], c02[1] - c01[1])
    M = 2.0 * (c01[1] * v[0] - c01[0] * v[1])/(v[0]*v[0]+v[1]*v[1])
    v3 = (-v[1] * M, v[0] * M)
    b03 = atan2(v3[1], v3[0])/const_pi()
    t3 = 1 - t0 - k03/4.0 + 2*b03

    # Compute v4 and t4
    a01 = t0 - 0.5 + (3*k04 - 3*k14 - 2*k41)/24.0
    a02 = t0 + i0-11.0/6.0 + (3*k04 + 6*k02 - 3*k24 - 2*k42)/24.0
    r01, r02 = 0.5/sin(a01 * const_pi()), 0.5/sin(a02 * const_pi())
    c01 = (0.5, -0.5/tan(a01*const_pi()))
    c02 = (r02*sin((a02 + 1.0/3.0)*const_pi()), -r02*cos((a02 + 1.0/3.0)*const_pi()))
    v = (c02[0] - c01[0], c02[1] - c01[1])
    M = 2.0 * (c01[1] * v[0] - c01[0] * v[1])/(v[0]*v[0]+v[1]*v[1])
    v4 = (-v[1] * M, v[0] * M)
    b04 = atan2(v4[1], v4[0])/const_pi()
    t4 = 1 - t0 - k04/4.0 + 2*b04

    # Compare v3,t3 and v4,t4
    t34,t43 = t3 + k34/5.0, t4 + k43/6.0
    b34 = atan2(v4[1]-v3[1], v4[0]-v3[0])/const_pi()

    # Compare and account for small errors in round-off
    lhs, rhs = (t34 + t43, 1 + 2 * b34)
    diff = mod((lhs - rhs) if lhs > rhs else (rhs - lhs), 2)
    epsilon = 0.000001
    if (diff < epsilon or diff > 2-epsilon):
        return True      # Found a valid assignment

for k0 in permutations(range(1,4)):
    for k1 in permutations(range(1,4)):
        for k2 in permutations(range(1,4)):
            for k3 in permutations(range(1,5),r=3):
                for k4 in permutations(range(1,6),r=3):
                    for (i0,i1,i2) in product(range(0,2), repeat=3):
                        with precision(100):
                            if match(k0,k1,k2,k3,k4,i0,i1,i2):
                                print "Valid match found."

```

Tab. 1: Python code to verify  $G_8$  is non-Lombardi

420 **Corollary 4.2.** *There are an infinite number of biconnected non-Lombardi graphs.*

421 *Proof.* Let  $G$  be formed from a graph  $G'$ , having at least two degree-one vertices  $u$  and  $v$  that do not share a com-
422 mon neighbor, by merging  $u$  and  $v$  and creating a degree-two vertex  $w$ . If  $G$  is Lombardi, then so is  $G'$  as we can
423 take a Lombardi drawing of  $G$ , split  $w$ , and place  $u$  and  $v$  on the arcs between  $w$  and its respective neighbor, and
424 still maintain a valid Lombardi drawing. Thus, we can take any collection of disjoint copies of  $G_8$  and combine
425 degree-one vertices as described above to form a biconnected non-Lombardi graph.  $\square$

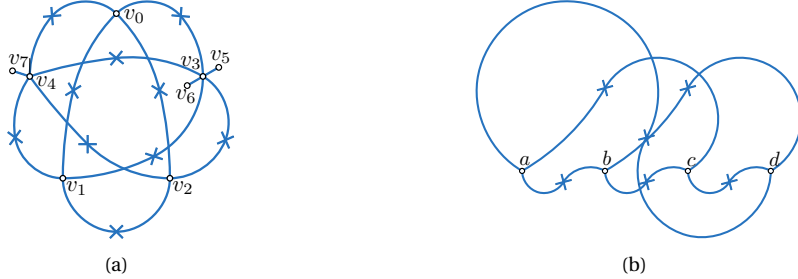


Fig. 16: (a) An example 2-Lombardi drawing of  $G_8$ . The bend points (not all of which are necessary) are shown with crossed marks. (b) An example 2-Lombardi drawing of  $K_4$  with the vertices placed on a line and tangents oriented to force numerous inflection points.

## 4.2 Smooth 2-Lombardi Drawings

If we want to draw Lombardi style drawings for any given graph we have to relax one of the two requirements that specify Lombardi drawings. Ideally, we would like to avoid relaxing the requirement that edges have perfect angular resolution. Fortunately, as the following theorem shows, we can achieve a “close-to-Lombardi” drawing for any graph if we allow two circular arcs per edge.

**Theorem 4.3.** *Every graph has a smooth 2-Lombardi drawing. Furthermore, the vertices can be chosen to be in any fixed position.*

*Proof.* Starting with the given graph  $G$ , subdivide every edge by dividing it in two and adding a “dummy” vertex incident to these two new edges. Let  $G_2$  denote the resulting 2-degenerate graph. Duncan et al. [14] show that any 2-degenerate graph has a Lombardi drawing. Furthermore, each dummy vertex of  $G_2$  that was added to subdivide an edge of  $G$  has degree 2; hence, in a Lombardi drawing of  $G_2$  the edges incident on each such dummy vertex have tangents that meet at 180 degrees. Thus, when we consider these two circular arcs of  $G_2$  as a single edge of  $G$  they define a smooth two-arc edge. See Figure 16(a).

The 2-degenerate drawing algorithm orders the vertices in such a way that each vertex has at most two earlier neighbors; it places vertices with zero or one previous neighbor freely, but vertices with two previous neighbors are constrained to lie on a circular arc. For  $G_2$ , we can choose an ordering in which only the dummy vertices have two previous neighbors; therefore, the vertices of  $G$  can have any initial placement.  $\square$

As Figure 16(b) illustrates, although we can place the vertices in any position with any initial orientation, an arc’s smooth bend point might be an inflection point.

## 5 Planar $k$ -Lombardi Drawings

We have seen that with  $k$ -Lombardi drawing we can represent many more graphs than with the standard Lombardi drawing. Planar Lombardi drawings, however are limited to only a subset of the planar graphs. In this section we investigate the combination of planarity and  $k$ -Lombardi drawing.<sup>3</sup>

### 5.1 Planar 2-Lombardi pointed drawings for planar graphs

We now show that every planar graph allows a planar 2-Lombardi drawing with pointed joints. The approach is similar to the previous section, but the drawing method inside the disks is different.

Assume that we are given a circle  $C$ , a set  $P$  of  $n$  points on  $C$ , and four integers  $n_1, n_2, n_3, n_4$  that sum up to  $n$  and that satisfy the inequalities  $\lfloor n/4 \rfloor \leq n_i \leq \lceil n/4 \rceil$  and  $\lfloor n/2 \rfloor \leq n_i + n_{(i+1) \bmod 4} \leq \lceil n/2 \rceil$ . We will show (Lemma 5.2)

<sup>3</sup> In the conference version [13] of this paper we proved that planar graphs of maximum degree 3 have a planar smooth 2-Lombardi drawing. We dropped this result as in the meantime Eppstein [17] showed that these graphs are actually even planar Lombardi.

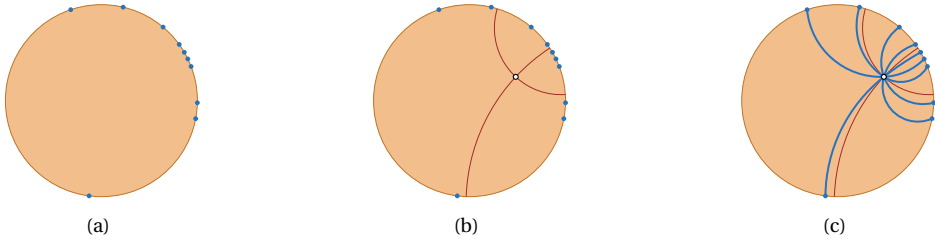


Fig. 17: (a) A disk with a set of connection points on its boundary. (b) A placement for the vertex in the disk that divides the connection points into four quadrants. (c) The actual connections are not fixed, and guaranteed to not intersect.

454 that there exist two circles  $A$  and  $B$  disjoint from  $P$  such that  $A$ ,  $B$ , and  $C$  are pairwise perpendicular and such that  
 455  $A$  and  $B$  subdivide  $P$  into four sets of cardinality  $n_1, n_2, n_3$  and  $n_4$ .

456 It is convenient to begin with a continuous analogue of the lemma. We define a *smooth* probability distribution  
 457 on  $C$  to be a distribution that assigns a nonzero probability to any arc of  $C$ , such that arbitrarily short arcs have a  
 458 probability that approaches zero.

459 **Lemma 5.1.** *Let  $C$  be a circle, and  $\Pi$  be a smooth probability distribution on  $C$ . Then there exist two circles  $A$  and  $B$   
 460 such that  $A$ ,  $B$ , and  $C$  are pairwise perpendicular and such that the four arcs of  $C$  formed by its crossing points with  
 461  $A$  and  $B$  each have probability  $1/4$  under distribution  $\Pi$ .*

462 *Proof.* We may view  $A$  and  $B$  as arcs inside  $C$  (ignoring part of the circles) that end perpendicular to  $C$ , and cross  
 463 each other at a  $90^\circ$  angle. Figure 17(b) illustrates this. We can consider  $C$  as a hyperbolic plane in the Poincaré disc  
 464 model. With this interpretation,  $A$  and  $B$  represent perpendicular lines in this plane, and  $C$  is the set of points at  
 465 infinity.

466 Let  $X$  be a line that divides  $C$  into two arcs that each have probability  $1/2$ . There exists a (combinatorially)  
 467 unique line  $Y$  perpendicular to  $X$  that also divides  $C$  into two arcs with probability  $1/2$ . The four arcs formed by  
 468 the crossings of  $C$  with both  $X$  and  $Y$  necessarily have probabilities  $1/4 + x, 1/4 - x, 1/4 + x, 1/4 - x$  for some  $x$ , but it  
 469 will not necessarily be the case that  $x = 0$ . Now, we conceptually rotate  $X$  and  $Y$ , keeping them perpendicular and  
 470 maintaining invariant the property that each of  $X$  and  $Y$  divides  $P$  into two equal-probability arcs. As we do so,  $x$   
 471 will change continuously; by the time we rotate  $X$  into the position initially occupied by  $Y$ ,  $x$  will have negated its  
 472 original value. Therefore, by the intermediate value theorem, there must be some position during the rotation at  
 473 which  $x = 0$ . The circles  $A$  and  $B$  formed by extending  $X$  and  $Y$  outside the model of the hyperbolic plane, for this  
 474 position, satisfy the statement of the lemma.  $\square$

475 **Lemma 5.2.** *Let  $C$  be a circle, and  $P$  be a set of  $n$  points on  $C$ . Additionally suppose that the four integers  $n_1, n_2, n_3, n_4$   
 476 sum up to  $n$  and satisfy the inequalities  $\lfloor n/4 \rfloor \leq n_i \leq \lceil n/4 \rceil$  and  $\lfloor n/2 \rfloor \leq n_i + n_{(i+1) \bmod 4} \leq \lceil n/2 \rceil$ . Then there exist two  
 477 circles  $A$  and  $B$  disjoint from  $P$  such that  $A$ ,  $B$ , and  $C$  are pairwise perpendicular and such that  $A$  and  $B$  subdivide  
 478  $P$  into four sets of cardinality  $n_1, n_2, n_3$  and  $n_4$ .*

479 *Proof.* For any sufficiently small number  $\epsilon$ , let  $\Pi_\epsilon$  be the smooth probability distribution formed by adding a uniform  
 480 distribution with total probability  $\epsilon$  on all of  $C$  to a uniform distribution with total probability  $1 - \epsilon$  on the  
 481 points within distance  $\epsilon$  of  $P$ . Apply Lemma 5.1 to  $\Pi_\epsilon$ , and let  $A$  and  $B$  be pairs of circles obtained in the limit as  $\epsilon$   
 482 goes to zero. Then (if points on the boundaries of the arcs are assigned fractionally to the two arcs they bound as  
 483 appropriate) the number of points assigned to each of the four arcs of  $C$  disjoint from  $A$  and  $B$  is exactly  $n/4$ .

484 Next, rotate  $A$  and  $B$  by a small amount around their crossing point (as hyperbolic lines), that is, preserving  
 485 their perpendicularity to each other and to  $C$ . This rotation causes them to become disjoint from all points in  $P$ .  
 486 Each of the four arcs determined by the four crossing points, and each of the two longer arcs determined by two of  
 487 the four crossing points, gains or loses only a fractional point by this rotation, so the inequalities  $\lfloor n/4 \rfloor \leq n_i \leq \lceil n/4 \rceil$   
 488 and  $\lfloor n/2 \rfloor \leq n_i + n_{(i+1) \bmod 4} \leq \lceil n/2 \rceil$  (where  $n_i$  denotes the size of the  $i$ th arc) remain true after this rotation.  
 489 However, there may be more than one solution to this system of inequalities, so we analyze cases according to the

490 value of  $n$  modulo four to determine that the solution obtained geometrically in this way matches the values of  $n_i$   
491 given to us in the lemma:

- 492 • If  $n = 0 \pmod{4}$ , the only choice for the values of  $n_i$  is that all of them are equal to  $n/4$ .
- 493 • If  $n = 1 \pmod{4}$ , then three of the  $n_i$  must be  $\lfloor n/4 \rfloor$  and one must be  $\lceil n/4 \rceil$ . By exchanging the roles of  $A$  and  $B$  as necessary we can ensure that the quadrant that is supposed to contain the larger number of points is the one that actually does.
- 496 • If  $n = 2 \pmod{4}$  then the only solution to the inequalities is that two opposite quadrants have  $\lfloor n/4 \rfloor$  points and the other two have  $\lceil n/4 \rceil$ . Again, by exchanging  $A$  and  $B$  if necessary we can ensure that the correct two quadrants have the larger number of points.
- 499 • If  $n = 3 \pmod{4}$ , then one of the  $n_i$  must be  $\lfloor n/4 \rfloor$  and the remaining three must be  $\lceil n/4 \rceil$ . Again, by exchanging the roles of  $A$  and  $B$  as necessary we can ensure that the quadrant that is supposed to contain the smaller number of points is the one that actually does.

502 Thus, in each case the partition satisfies the requirements of the lemma.  $\square$

503 Now, we apply the lemma to draw the neighbourhood of each vertex inside a circle in such a way that their  
504 half-edges can be connected into 2-Lombardi edges.

505 **Lemma 5.3.** *Given a circle  $C$  and a set  $P$  of  $n$  points on  $C$ , there exists a point  $p$  in  $C$  such that we can draw  $n$  edges  
506 from  $p$  to the points in  $P$  as circular arcs that lie completely inside  $C$ , do not cross each other, and meet in  $p$  at  $360/n^\circ$   
507 angles.*

508 *Proof.* Draw  $n$  ports around a point with equal angles, and draw two perpendicular lines through the point (not  
509 coinciding with any ports), and count the number of points in each quadrant. Let these numbers be  $n_1, \dots, n_4$  and  
510 find two circles  $A$  and  $B$  as in Lemma 5.2. Then we place  $p$  at their intersection point inside  $C$ . Now orient the  
511 ports at  $p$  such that each quadrant has the correct number of ports.

512 Within any quadrant, there is a circular arc tangent to  $C$  at the point where it is crossed by  $B$ , and tangent to  $A$   
513 at point  $p$ ; this can be seen by using a Möbius transformation to transform  $A$  and  $B$  into a pair of perpendicular  
514 lines, after which the desired arc has half the radius of  $C$ . By the intermediate value theorem, there are two circular  
515 arcs from  $p$  to any point  $q$  on the boundary arc of the quadrant that remain entirely within the quadrant and are  
516 tangent to  $A$  and  $B$  respectively. By a second application of the intermediate value theorem, there is a unique  
517 circular arc that connects  $p$  to each connection point on the boundary of  $C$ , such that the outgoing direction at  $p$   
518 matches the port, and such that the arc remains entirely within its quadrant.

519 Any two arcs that belong to the same quadrant belong to two circles that cross at  $p$  and at one more point.  
520 Whether that second crossing point is inside or outside of the quadrant can be determined by the relative ordering  
521 of the two arcs at  $p$  and on the boundary of the quadrant. However, since the ordering of the ports and of the  
522 connection points is the same, none of the crossings of these circles are within the quadrant, so no two arcs cross.

523 524 Figure 17(c) illustrates the lemma. We now have all ingredients to prove the main result of this section.  $\square$

525 **Theorem 5.4.** *Every planar graph has a planar pointed 2-Lombardi drawing.*

526 *Proof.* We first obtain a touching-circles representation of a the given graph  $G$  using the Koebe–Andreev–Thurston  
527 theorem. Each vertex  $v$  in  $G$  is represented by a circle  $C$ ; place  $v$  together with arcs connecting it to the set of  
528 contact points on  $C$  using Lemma 5.3. The arcs meet up at the contact points to form (non-smooth) 2-Lombardi  
529 edges.  $\square$

530 **5.2 Smooth 3-Lombardi planar realization for planar graphs**

531 Note that the 2-Lombardi planar realization of the previous section has non-smooth bends in each edge. As we  
532 now show, every planar graph also has a smooth 3-Lombardi drawing.

533 It seems likely that every planar graph  $G$  has a smooth 3-Lombardi drawing formed by perturbing each edge  
534 of a straight-line drawing of  $G$  into a curve formed by two very small circular arcs near each endpoint of the edge,  
535 connected to each other by a straight segment. However, the details of this construction are messy. An alternative  
536 construction is much simpler, once Theorem 5.4 is available:

537 **Theorem 5.5.** *Every planar graph has a planar smooth 3-Lombardi drawing.*

538 *Proof.* Find a pointed planar 2-Lombardi drawing by Theorem 5.4. For each pointed bend of the drawing formed  
539 by two circular arcs  $a_1$  and  $a_2$ , replace the bend by a third circular arc tangent to both  $a_1$  and  $a_2$ , with the two  
540 points of tangency close enough to the bend to avoid crossing any other edge.  $\square$

541 **6 Conclusions**

542 We have proven several new results about planarity of Lombardi drawings and about classes of graphs that can  
543 be drawn with  $k$ -Lombardi drawings rather than Lombardi drawings. However, several problems remain open,  
544 including the following:

- 545 1. Characterize the subclass of planar graphs that are planar Lombardi. In particular, are all outerplanar graphs  
546 planar Lombardi? What is the complexity of testing Lombardi planarity?
- 547 2. Characterize the subclass of planar graphs that have smooth 2-Lombardi planar realizations.
- 548 3. Address the questions of the area and resolution needed for Lombardi drawings of graphs.
- 549 4. Finally, it would be valuable to investigate the readability of the planar and  $k$ -Lombardi drawings created  
550 by our algorithms, and more specifically, which of our two methods to create smooth 3-Lombardi planar  
551 drawings yields visually more pleasing results.

552 **Acknowledgments**

553 This research was supported in part by the National Science Foundation under grants 0830403, CCF-1423411,  
554 and CCF-1712119, by the Office of Naval Research under MURI grant N00014-08-1-1015, by the German Re-  
555 search Foundation under grant NO 899/1-1, and by the Dutch National Science Foundation (NWO) under grant  
556 639.021.123.

557 **References**

- 558 [1] O. Aichholzer, W. Aigner, F. Aurenhammer, K. Č. Dobiášová, B. Jüttler, and G. Rote. Triangulations with  
559 circular arcs. In M. van Kreveld and B. Speckmann, editors, *Graph Drawing (GD'11)*, volume 7034 of *LNCS*,  
560 pages 296–307. Springer, 2012.
- 561 [2] M. J. Alam, M. A. Bekos, M. Kaufmann, S. G. Kobourov, P. Kindermann, and A. Wolff. Smooth orthogonal  
562 drawings of planar graphs. In A. Pardo and A. Viola, editors, *Theoretical Informatics (LATIN'14)*, volume 8392  
563 of *LNCS*, pages 144–155. Springer, 2014.
- 564 [3] J. S. Andrade, Jr., H. J. Herrmann, R. F. S. Andrade, and L. R. da Silva. Apollonian networks: Simultaneously  
565 scale-free, small world, Euclidean, space filling, and with matching graphs. *Physics Review Letters*, 94:018702,  
566 2005.
- 567 [4] D. N. Arnold and J. Rogness. Möbius Transformations Revealed. *Notices of the AMS*, 55(10):1226–1231, 2008.

- 568 [5] M. A. Bekos, H. Förster, and M. Kaufmann. On smooth orthogonal and octilinear drawings: Relations,  
 569 complexity and Kandinsky drawings. In F. Frati and K.-L. Ma, editors, *Graph Drawing and Network  
 570 Visualization (GD'17)*, volume 10692 of *LNCS*, pages 169–183. Springer, 2018.
- 571 [6] M. A. Bekos, M. Gronemann, S. Pupyrev, and C. N. Raftopoulou. Perfect smooth orthogonal drawings. In  
 572 *Information, Intelligence, Systems and Applications (IISA'14)*, pages 76–81, 2014.
- 573 [7] M. A. Bekos, M. Kaufmann, S. G. Kobourov, and A. Symvonis. Smooth orthogonal layouts. *J. Graph  
 574 Algorithms Appl.*, 17(5):575–595, 2013.
- 575 [8] U. Brandes and D. Wagner. Using graph layout to visualize train interconnection data. In S. Whitesides,  
 576 editor, *Graph Drawing*, volume 1547 of *LNCS*, pages 44–56. Springer, 1998.
- 577 [9] C. C. Cheng, C. A. Duncan, M. T. Goodrich, and S. G. Kobourov. Drawing planar graphs with circular arcs.  
 578 *Discrete Comput. Geom.*, 25(3):405–418, 2001.
- 579 [10] R. Chernobelskiy, K. Cunningham, M. T. Goodrich, S. G. Kobourov, and L. Trott. Force-directed  
 580 Lombardi-style graph drawing. In M. van Kreveld and B. Speckmann, editors, *Graph Drawing (GD'11)*,  
 581 volume 7034 of *LNCS*, pages 320–331. Springer Berlin Heidelberg, 2012.
- 582 [11] G. Di Battista and L. Vismara. Angles of planar triangular graphs. *SIAM J. Discrete Math.*, 9(3):349–359, 1996.
- 583 [12] M. Dickerson, D. Eppstein, M. T. Goodrich, and J. Y. Meng. Confluent drawings: Visualizing non-planar  
 584 diagrams in a planar way. *J. Graph Algorithms Appl.*, 9(1):31–52, 2005.
- 585 [13] C. A. Duncan, D. Eppstein, M. T. Goodrich, S. G. Kobourov, and M. Löffler. Planar and poly-arc Lombardi  
 586 drawings. In M. van Kreveld and B. Speckmann, editors, *Graph Drawing (GD'11)*, volume 7034 of *LNCS*,  
 587 pages 308–319. Springer Berlin Heidelberg, 2012.
- 588 [14] C. A. Duncan, D. Eppstein, M. T. Goodrich, S. G. Kobourov, and M. Nöllenburg. Lombardi drawings of  
 589 graphs. *J. Graph Algorithms and Applications*, 16(1):85–108, 2012.
- 590 [15] C. A. Duncan, D. Eppstein, M. T. Goodrich, S. G. Kobourov, and M. Nöllenburg. Drawing trees with perfect  
 591 angular resolution and polynomial area. *Discrete and Computational Geometry*, 49(2):157–182, 2013.
- 592 [16] A. Efrat, C. Erten, and S. G. Kobourov. Fixed-location circular arc drawing of planar graphs. *J. Graph  
 593 Algorithms Appl.*, 11(1):145–164, 2007.
- 594 [17] D. Eppstein. A Möbius-invariant power diagram and its applications to soap bubbles and planar Lombardi  
 595 drawing. *Discrete and Computational Geometry*, 52:515–550, 2014.
- 596 [18] D. Eppstein. Simple recognition of Halin graphs and their generalizations. *J. Graph Algorithms Appl.*,  
 597 20(2):323–346, 2016.
- 598 [19] D. Eppstein, M. Löffler, E. Mumford, and M. Nöllenburg. Optimal 3D angular resolution for low-degree  
 599 graphs. In U. Brandes and S. Cornelsen, editors, *Graph Drawing*, volume 6502 of *LNCS*, pages 208–219.  
 600 Springer, Heidelberg, 2011.
- 601 [20] B. Finkel and R. Tamassia. Curvilinear graph drawing using the force-directed method. In J. Pach, editor,  
 602 *Graph Drawing*, volume 3383 of *LNCS*, pages 448–453. Springer, Heidelberg, 2005.
- 603 [21] A. Garg and R. Tamassia. Planar drawings and angular resolution: Algorithms and bounds. In J. van Leeuwen,  
 604 editor, *Algorithms - ESA '94*, volume 855 of *LNCS*, pages 12–23. Springer, Heidelberg, London, UK, 1994.
- 605 [22] M. T. Goodrich and C. G. Wagner. A framework for drawing planar graphs with curves and polylines. *Journal  
 606 of Algorithms*, 37(2):399–421, 2000.

- 607 [23] C. Gutwenger and P. Mutzel. Planar polyline drawings with good angular resolution. In S. Whitesides, editor,  
 608     *Graph Drawing*, volume 1547 of *LNCS*, pages 167–182. Springer, Heidelberg, London, UK, 1998.
- 609 [24] W. Huang, P. Eades, S.-H. Hong, and H. Been-Lirn Duh. Effects of curves on graph perception. In *IEEE Pacific  
 610     Visualization Symposium (PacificVis'16)*, pages 199–203, 2016.
- 611 [25] G. Kant. Drawing planar graphs using the canonical ordering. *Algorithmica*, 16:4–32, 1996.
- 612 [26] A. Lhuillier, C. Hurter, and A. Telea. State of the art in edge and trail bundling techniques. *Computer Graphics  
 613     Forum*, 36(3):619–645, 2017.
- 614 [27] M. Lombardi and R. Hobbs. *Mark Lombardi: Global Networks*. Independent Curators, 2003.
- 615 [28] M. Löffler and M. Nöllenburg. Planar Lombardi drawings of outerpaths. In W. Didimo and M. Patrignani,  
 616     editors, *Graph Drawing (GD'12)*, volume 7704 of *LNCS*, pages 561–562. Springer Berlin Heidelberg, 2013.  
 617     Poster abstract.
- 618 [29] S. Malitz and A. Papakostas. On the angular resolution of planar graphs. *SIAM J. Discrete Math.*,  
 619     7(2):172–183, 1994.
- 620 [30] H. C. Purchase, J. Hamer, M. Nöllenburg, and S. G. Kobourov. On the usability of Lombardi graph drawings.  
 621     In W. Didimo and M. Patrignani, editors, *Graph Drawing (GD'12)*, volume 7704 of *LNCS*, pages 451–462.  
 622     Springer Berlin Heidelberg, 2013.
- 623 [31] K. Xu, C. Rooney, P. Passmore, D.-H. Ham, and P. H. Nguyen. A user study on curved edges in graph  
 624     visualization. *IEEE Trans. Visualization and Computer Graphics*, 18(12):2449–2456, 2012.